

Thermophoretic Sensors for Combustion Formed Nanoparticles

Mario Commodo^{*a}, Gianluigi De Falco^b, Patrizia Minutolo^a, Andrea D'Anna^b

^aIstituto di Ricerche sulla Combustione, CNR, P.le Tecchio 80, 80125 Napoli, Italy

^bDipartimento di Ingegneria Chimica, dei Materiali e della Produzione Industriale – Università degli Studi di Napoli Federico II, P.le Tecchio 80, 80125 Napoli, Italy
commodo@irc.cnr.it

It is well established that ultrafine carbonaceous particles represent the major source of carbon aerosols in the atmosphere, and their formation has been intensively investigated over the last decades due to their negative effects on human health and environment. Moreover, combustion-formed nanoparticles represent a broad class of compounds since they can be highly variable in terms of size, chemical composition, morphology and optical properties. In the light of the above, the development of highly sensitive, costly effective combustion aerosols sensors, capable to give both qualitative and quantitative information is needed. In this work, thermocouple particle densitometry (TPD) technique, which is based on the thermophoretic sampling principle, has been carried out to detect nanoparticles produce in a slightly sooting laminar premixed flame at different height above the burner (HAB). With this technique, the particle emissivity and the total particulate volume fraction have been obtained and results are compared with the ones determined by on-line measurements using a Scanning Mobility Particle Sizer system (SMPS). The good agreement between results obtained with the two independent measurements demonstrates that transient-thermocouple measurement is a powerful technique to detect the total particulate volume fraction, together with particle emissivity. In addition, thermophoretic sampling has been adopted for the collection and electrical characterization of combustion nanoparticles with different graphitization degree. This work demonstrates that the feasibility of such an approach can be useful for the development of conductometric combustion aerosol sensors.

1. Introduction

The emission of carbon particles from both stationary and automotive combustion systems has long been of concern for their negative effects on the human health, on the environment and for the climate change (Lighty et al., 2000). In addition, the formation and the emission of carbonaceous aerosols is a clear marker of a not efficient combustion process. Indeed, soot particles are generated from the incomplete combustion of hydrocarbons as a result of a complex network of chemical and physical processes. In fuel-rich flames, the thermal decomposition of hydrocarbon fuel molecules promotes the formation of radical products which later recombine forming benzene and polycyclic aromatic hydrocarbons (PAHs) onward in the post-flame region (Richter and Howard, 2000). Once formed, PAHs participate to the soot formation process, being the building blocks of the solid soot particles. The chemical and physical properties of the so generated soot particles depend on the combustion conditions (D'Anna, 2009) and on the fuel chemical composition (Carbone et al., 2010). Combustion formed carbon nanoparticles are typically divided into two major classes based on the bimodal shape of the particle size distributions (PSDs), which is typically encountered in many combustion systems. These two classes are: a nucleation mode whose particles size are of the order of 2-3 nm and a primary soot mode whose particles sizes span from few nanometers up to tens of nanometers. These two classes of particles also have different optical properties, chemical and structural characteristics (Commodo et al., 2015).

In this work, carbon nanoparticles formed in a slightly sooting laminar premixed flame have been preliminary investigated by scanning mobility particle sizer (SMPS) for measuring PSD evolution along the flame axis, and by thermophoretic particle densitometry (TPD) for particle volume fraction and physicochemical

characterization measurements. Off-line Raman spectroscopy, has been also implemented in order to characterize the carbonaceous material deposited on the thermocouple and to support the results obtained from the TPD analysis. In addition, the feasibility of detecting and analysing combustion aerosol nanoparticles by means of a conductometric sensor has been investigated. Aerosols nanoparticles are again transported on the sensor surface by thermophoretic forces while the electrical properties of the collected material are used to gain both quantitative and qualitative information.

2. Experimental

2.1 Flame reactor configuration

A laminar premixed ethylene-air flame was stabilized on a McKenna burner with a diameter of 6 cm. The cold gas velocity was set at 10 cm/s and carbon to oxygen (C/O) was varied in order to produce a large variety of carbon nanoparticles with different sizes and chemical/structural characteristics. Measurements were performed also at various distances from the burner surface, herein referred to as height above the burner (HAB). Particle size distributions, PSDs, were measured on line by a scanning mobility particle sizer (SMPS) system. Following the procedure described in earlier works (see Commodo et al. 2015 and therein References), flame products were sampled by means of a high dilution tubular probe horizontally placed into the flame with its lateral sampling hole positioned downward, and connected to the inlet of the SMPS system. The experimental apparatus for flame nanoparticle formation and on-line collection is sketched in Fig. 1a.

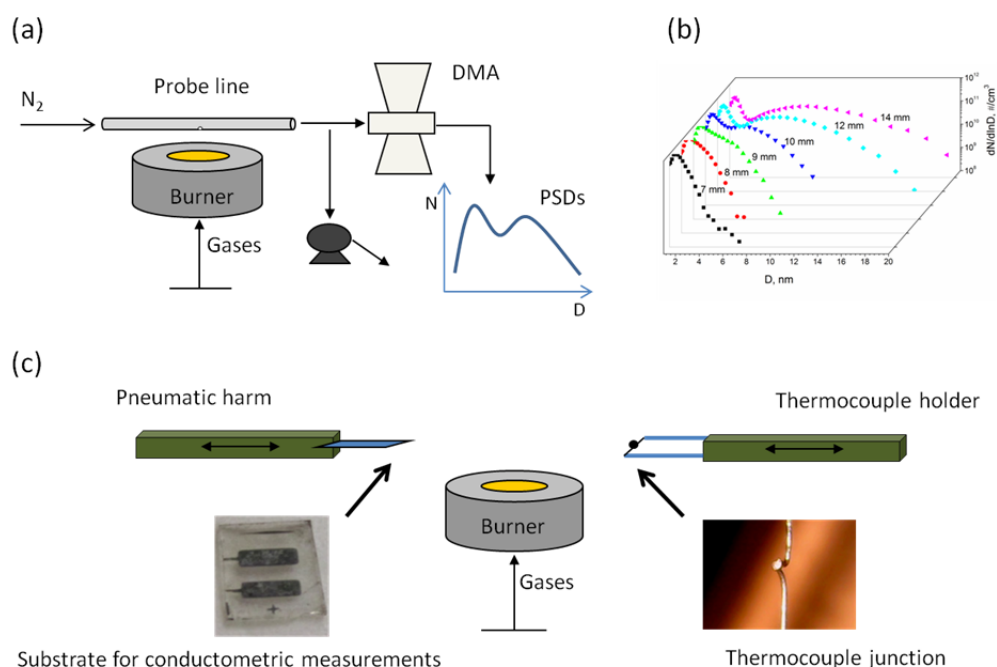


Figure 1. Experimental apparatus for on-line flame-formed nanoparticle analysis (a). PSDs measured along the axis at several HABs (b). Aerosol nanoparticle sampling methods for both off-line conductometric measurements (left side) and thermophoretic particle densitometry measurements (right side) (c).

2.2 Thermophoretic particle densitometry (TPD)

Following a previously developed methodology (McEnally et al., 1997), TPD measurements have been performed along the flame axis of a C/O=0.67 (equivalence ratio $\Phi=2.09$) laminar premixed flame, here named Flame 0, whose PSDs along at several HABs have been reported in Fig. 1b. Such measurements have been performed by means of an R-type thermocouple (Pt/Pt-13%Rh) with a spherical junction with a diameter of approximately 250 μm , shown on the right side of Fig.1c, using a rapid insertion procedure. Flame temperature was measured from the maximum of the temperature time profile applying corrections for radiation losses. The transient response of thermocouple, i.e. the temporal evolution of the temperature has been also recorded for about 3 min at each flame location and used to obtain information on both the particle volume fraction and the emissivity, i.e. the optical properties, of the carbonaceous materials deposited on the thermocouple. This study implements the procedure thoroughly described by McEnally et al., 1997 by including the evolution of carbon emissivity during the soot formation process.

Carbon particles deposited on the thermocouple junction were also analysed by Raman spectroscopy. Raman spectra were measured using a Horiba XploRA Raman microscope system equipped with a 100X objective (NA 0.9, Olympus). The laser source was a frequency doubled Nd:YAG laser ($\lambda=532$ nm, 12 mW maximum laser power at the sample). Details of the procedure are reported elsewhere (Minutolo et al., 2014).

2.3 Conductometric aerosol sensor

In many applications of gas sensing miniaturized solid-state devices are employed. In conductometric sensors the electrical properties between interdigital electrodes change after the deposition of chemical analytes. In particular, the conductometric sensors are particularly attractive, because of their simple structure and small dimension, ease of fabrication and low cost coupled with high sensitivity. In the current work we produced different flame-formed carbon nanoparticles from four experimental conditions, reported in Table 1.

Table 1: Investigated flame reactor parameters

	Flame 1	Flame 2	Flame 3	Flame 4
Equivalence ratio Φ	2.18	2.33	2.58	2.58
Cold gas velocity (cm/s)	10	10	10	10
Sampling position (mm)	6	10	10	15
Particle Residence time (ms)	6.4	14.4	13.7	25.2

Flame 1 is slightly-sooting, similar to Flame 0; the sampling position is located below the soot inception point as determined by visible luminosity. Flame 2 and Flames 3-4 are sooting and fully-sooting flames, respectively. In these flames, the sampling position is in the soot loading region, just after particle inception. Flame-formed nanoparticles were then collected by thermophoresis on quartz substrates provided with aluminum metal electrodes (the size was 5 x 2 mm and the distance between electrodes was 1 mm), see Fig. 1c left side, and their electrical behavior was investigated by measuring the I-V characteristics at room temperature using a Keithley Model 6487 picoammeter/voltage source (Keithley Instruments, USA), connected to a Signatone H-150 probe station (Signatone Corporation, USA). Again Raman spectroscopy was used to follow changes on the chemical/structural characteristics of the collected carbonaceous nanoparticles for the different flame conditions.

3. Results and discussion

The temporal evolution of the temperature has been recorded for about 3 min at each flame location. After a transient-response stage, junction temperature T_j reaches a maximum value, see Fig. 2, from which temperature of the gas T_g can be obtained by means of a quasi-steady energy balance at the junction (McEnally et al., 1997):

$$\varepsilon_j \sigma T_j^4 = \left(\frac{k_g Nu_j}{2d_j} \right) \cdot (T_g - T_j) \quad (1)$$

An analysis of the processes occurring during the measurement can be achieved by analysing the temporal evolution of the junction temperature together with its time first derivative, as reported in Figure 2. Particles in flame are driven by thermophoretic forces toward the junction and stick on its surface. This effect is negligible for the short time in which the maximum temperature is reached, but for longer times produces a decrease of the measured signal and two different regimes can be identified. During the first regime, called "variable-emissivity stage", which lasts up to $t = t^*$, temperature drops sharply since the emissivity of the junction ε_j is changing from the value of the pure metal to the value of the depositing particles. Usually, in less than 10 s ε_j reaches a constant value, which can be considered the emissivity of the particles covering the thermocouple. In the second regime, "variable-diameter stage", which occupies all $t > t^*$, T_j decreases more gradually and almost linearly and, consequently, its derivative assumes a constant value. This temperature decrease can be attributed to the increase of the size of the thermocouple bead for effect of continuous particle deposition. Consequently, it is a function of the thermophoretic flux and, hence, of the amount of particles in the combustion environment.

Particles emissivity values can be obtained by first identifying the time for which the first derivative of the temperature reaches a constant value, t^* . From the junction temperature in correspondence of this time value, $T(t^*)$ the emissivity of particles covering the thermocouple junction can be derived iteratively from Eq. 1. This procedure allows to obtain particle emissivity at various HAB, thus, to characterize combustion generated nanoparticles.

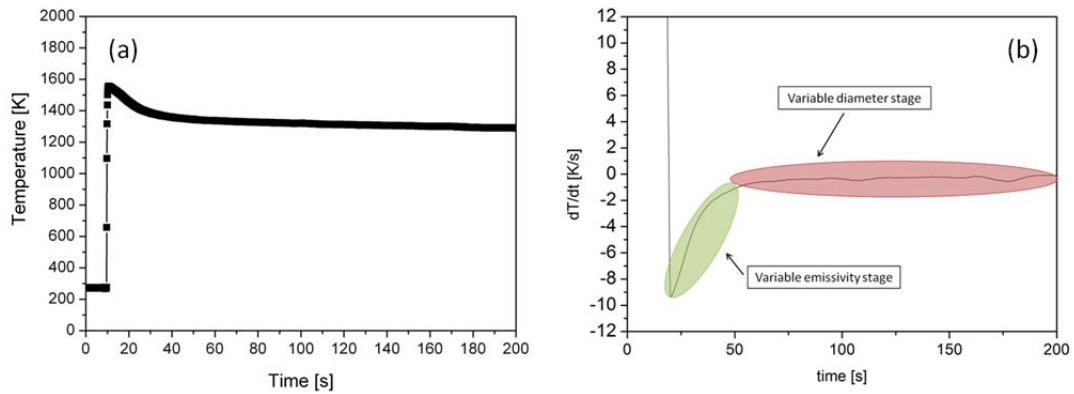


Figure 2. Temporal profile of thermocouple junction temperature measured at HAB=20 mm (a) and time first derivative (b).

Figure 3a shows the emissivity values of particles, formed at different HAB in Flame 0, obtained following the above procedure. In the lower zone, HAB < 4 mm, no carbonaceous particles are present in flame and, thus, the emissivity value is quite similar and constant to that of the clean thermocouple ($\epsilon \approx 0.2$). A value of emissivity $\epsilon \approx 0.5$ is measured in the soot pre-inception region of the flame (near 6 mm above the burner). It can be attributed to visible-transparent soot precursors, with mean sizes in the order of 2–3 nm, which are the only particles present in this flame region. Subsequently, the higher the HAB the higher the emissivity, and a value of emissivity $\epsilon > 0.8$ is measured in the sooting region (HAB > 10 mm). In this last zone, then, the higher concentration of soot is expected, and so emissivity tends to the limit of a black body ($\epsilon = 1$).

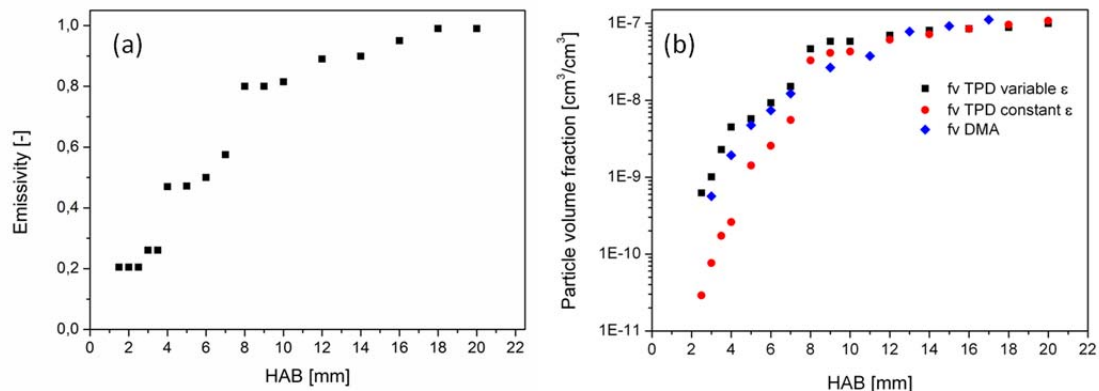


Figure 3. (a) Emissivity values calculated from TPD measurements as a function of HAB. (b) Particle volume fraction f_v calculated from SMPS measurements (blue rhombus), f_v calculated from TPD measurements with $\epsilon=0.95$ (red circles), and f_v calculated from TPD measurements with a variable ϵ (black squares).

Emissivity values derived with this new method were then used to calculate particle volume fraction in flame, as a function of HAB, using the procedure reported by McEnally et al., 1997. Particle volume fractions f_v , obtained from TPD measurements, were then compared to particle volume fractions calculated from the PSDFs measured by means of SMPS system at different height above the burner. Figure 3b reports a comparison between the f_v calculated from SMPS measurements, and the f_v calculated from TPD measurements using the variable emissivity reported in Fig. 3b. These two curves are in very good agreement. By contrast the f_v obtained by TPD measurements using the emissivity of soot particles, ($\epsilon=0.95$), underestimate the amount of particles produced in the soot pre-inception region of the flame, confirming that the emissivity of the soot precursors particles is lower than soot. Finally, Raman spectra were acquired for particles with emissivity of $\epsilon \approx 0.5$ and $\epsilon \approx 0.95$ respectively. In Figure 4 are reported the spectra relative to particles collected at two different HABs, namely 7 mm and 12 mm.

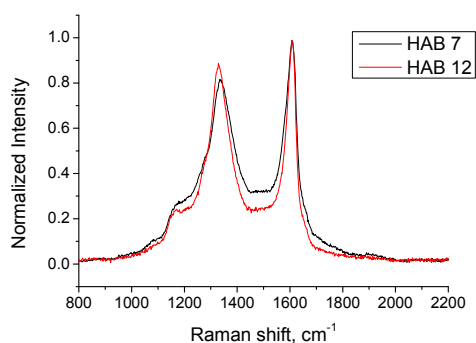


Figure 4. Raman spectra of nanoparticles deposited on thermocouple junction at HAB=7 mm (blue curve) and HAB=12 mm (red curve).

The most prominent features are the D and G peaks located approximately at 1340 cm^{-1} and 1600 cm^{-1} respectively. Both G and D peak are Raman active for hybridized sp^2 carbon, however the latter is only activated by an edge or a defect so that it is not observed in the Raman spectrum of the highly crystalline graphite and in a perfect graphene, whereas it appears in nano-crystalline graphite, due to edge effects, or in defected and amorphous carbon (Minutolo et al. 2014). The ratio of the D and G peak intensity has been widely used to estimate the in-plane correlation length of aromatic island, L_a . Tuinstra and Koenig (1970), first reported that the intensity of the D band is inversely proportional to L_a investigating the Raman spectrum of graphite and micro-crystalline graphite. Such functional dependence has been successively verified up to a minimum L_a of about 2 nm, where $I(\text{D})/I(\text{G})$ reaches a maximum value (Ferrari and Robertson 2001). When the effective crystallite size or the distance between defects further decreases, $I(\text{D})/I(\text{G})$ decreases to zero. For our carbon nanoparticles it is well ascertained that average values of L_a are of the order of 1 nm (Minutolo et al. 2014, Commodo et al., 2015) and thus the correct regime in which evaluate variations in the sampled carbon nanoparticles is the second one. Based on this and considering the Raman spectra reported in Fig. 4 it results that carbon nanoparticle collected by the thermocouple at 12 mm ($\epsilon \approx 0.95$) present a larger degree of graphitization as compared to those collected at 7 mm ($\epsilon \approx 0.5$), thus confirming and possibly explaining the observed different optical properties.

To investigate how the degree of graphitization in carbon compounds affects conductivity I/V characteristic has been measured as described previously.

Figure 5a reports a typical I/V plot measured on nanoparticles collected from Flame 4 condition. The curve is symmetrical and exhibits a non-linearity which addresses to a non-ohmic electrical behaviour.

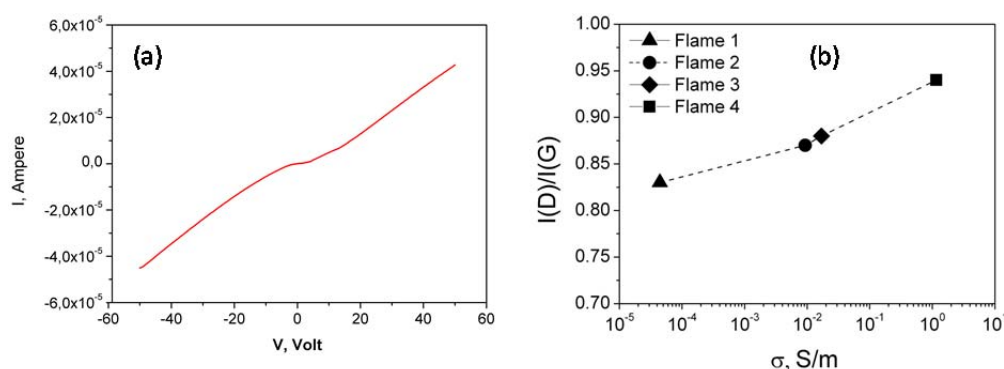


Figure 5. Typical I-V plot of flame-formed nanoparticles deposited via thermophoresis in conductrometric measurements (a). $I(\text{D})/I(\text{G})$ ratio as obtained by Raman spectroscopy of the deposited nanoparticles for different flame conditions vs. electrical conductivity (b).

The electrical conductivity σ of the particles deposited on the conductometric sensor has been estimated from Equation 2:

$$\sigma = G \left(\frac{1}{d \cdot \delta} \right) \quad (2)$$

where G is the electrical conductance, calculated as the slope of the I-V curves in the interval between 20 and 50 V, δ is the thickness of the deposit estimated from light absorption spectra by means of Beer-Lambert law, l is the distance between the electrodes ($l=0.1$ cm) and d is the length of each electrode ($d=0.5$ cm). Figure 5b shows the electrical conductivity, σ , compared with the $I(D)/I(G)$ ratio derived from Raman spectra for the four carbon materials. The increase of conductivity from Flame 1 to Flame 4 sample follows the increase of $I(D)/I(G)$ and can be therefore correlated to the increase of the in plane size of graphitic crystallites within the particles, L_a , in agreement with a graphitization trajectory of particles produced in flame. These results show how the structural and conductivity properties of flame formed carbon nanoparticles are connected, and they can be useful in order to realize conductometric sensors for the detection of particulate matter emitted from engines, and also to calibrate these sensors on the different classes of combustion-generated nanoparticles with different electrical behaviour.

4. Conclusion

Thermocouple particle densitometry (TPD) based on thermophoretic sampling has been carried out to detect nanoparticles at different height above the burner (HAB). With this technique, the particle emissivity and the total particulate volume fraction have been obtained and results are compared with the ones determined by on-line measurements using a Scanning Mobility Particle Sizer system (SMPS). Results show that moving from the base of the burner to high flame location, particle dimension and concentration increase as well as particle composition changes. An evidence of that is given by the emissivity values along the flame. Indeed, moving from the flame front emissivity values vary from the one of the clean thermocouple, i.e. $\epsilon=0.2$, to a value of $\epsilon=0.5$ reached in the particle inception zone where soot precursor particles are formed, to a value of $\epsilon=0.95$ in the soot phase zone. Using these emissivity values, the soot volume fraction obtained with the TPD method is quite similar to that one obtained from on-line measurement using the SMPS system. The good agreement between results obtained with the two independent measurements demonstrates that transient-thermocouple measurement is a powerful technique to detect the total particulate volume fraction in addition to its emissivity. In addition, thermophoretic sampling has been adopted for the collection and electrical characterization of combustion nanoparticles with different graphitization degree in order to gain information on the feasibility of such an approach for the development of conductometric combustion aerosol sensors.

Acknowledgments

This work was financially supported by Accordo MSE-CNR- Ricerca di sistema elettrico nazionale- Project "Miglioramento dell'efficienza energetica dei sistemi di conversione locale di energia" PAR 2013-2014

References

- Carbone F., Beretta F., D'Anna A., High-temperature ultrafine aerosol formation burning low quality fuels, *Chemical Engineering Transactions*, 22, 245-250, (2010).
- Commodo M., De Falco G., Bruno A., Borriello C., Minutolo P., D'Anna A., Physicochemical evolution of nascent soot particles in a laminar premixed flame: from nucleation to early growth, *Combust. Flame* 162 (2015) 3854–3863.
- D'Anna A., Combustion-Formed Nanoparticles, *Proc. Combust. Inst.* 32 (2009) 593–613.
- Ferrari A.C., Robertson J., Resonant Raman spectroscopy of disordered, amorphous, and diamond like carbon. *Phys Rev B* 64 (2001) 075414–26.
- Lighty J.S., Veranth J.M., Sarofim A.F., Combustion Aerosols: Factors Governing Their Size and Composition and Implications to Human Health, *J. Air Waste Manag. Assoc.* 50 (2000) 1565-1618.
- McEnally C.S., Koylu U.O., Pfefferle L.D., Rosner D.E., Soot volume fraction and temperature measurements in laminar nonpremixed flames using thermocouples, *Combust. Flame* 109 (1997) 701–720.
- Minutolo P., Commodo M., Santamaria A., De Falco G., D'Anna A., Characterization of flame-generated 2-D carbon nano-disks, *Carbon* 68 (2014) 138-148.
- Richter H., Howard J.B., Formation of polycyclic aromatic hydrocarbons and their growth to soot-a review of chemical reaction pathways, *Prog. Energy. Combust. Sci.* 26 (2000) 565–608.
- Tuinstra F., Koenig J.L., Raman spectrum of graphite, *J Chem. Phys.* 53 (1970) 1126–1131.